Heat Transfer in Reacting Systems: Heat Transfer To Nitrogen Dioxide Gas Under Turbulent Pipe Flow Conditions

WALTER F. KRIEVE and DAVID M. MASON

Jet Propulsion Laboratory, California Institute of Technology, Pasadena, California

Heat transfer rates of both heating and cooling for dissociating nitrogen dioxide gas were experimentally measured under turbulent pipe-flow conditions. The range of the average Reynolds numbers for which these measurements were made was from 6,700 to 22,000. Thermal flux at the inside surfaces of the tubes ranged from 300 to 8,400 B.t.u./hr.-sq. ft. for heating and cooling. Wall temperatures of the heater section were varied from 100° to 400°F. and those of the cooler section were varied from 70° to 140°F. Mixed mean bulk gas temperatures for both heating and cooling were in the range 72° to 190°F. Radial velocity and temperature profiles were measured at various longitudinal positions in the heater section.

For this equilibrium gas mixture heat transfer coefficients as high as 14 times those for the gas under frozen equilibrium conditions were obtained. Correlations which should be generally applicable to equilibrium reacting systems have been determined from the experimental data.

The rates of heat transfer processes can be unusually high in gaseous systems that undergo equilibrium type of homogeneous dissociation with a large energy of dissociation. If, for an endothermic or exothermic equilibrium type of homogeneous reacting gas, the reaction times are small compared with diffusion times, chemical equilibrium effectively prevails throughout the system and the values of thermal properties such as thermal conductivity and specific heat of the system will be unusually high and will be nonmonotonic functions of temperature. It is primarily the fact that thermal properties such as thermal conductivity and heat capacity of such systems are high that gives rise to unusually high heat transfer rates.

Detailed quantitative analysis of the behavior of thermal properties of reacting systems is given in the literature (*4, 7*). Qualitatively however it may be noted that in the case of the measurement of the heat capacity of an endothermic equilibrium type of gas system for example a given addition of thermal energy to the system the temperature rise will be low owing to the fact that there is a shift in equilibrium which absorbs energy. Since the temperature rise is low for a given addition of heat, the measured heat capacity will be large. The thermal conductivity is related to the heat capacity by the kinetic theory (*4, 7*), and thus it would also assume high values in reacting systems.

Nitrogen dioxide undergoes endothermic dissociation in the range 75 to 300°F.:

$$N_2O_4 \rightleftharpoons 2NO_2 \quad \Delta H_r = 2.47 \times 10^4 \text{B.t.u./lb. mole at } 75°\text{F.} \quad (1)$$

At a pressure of 1 atm. the composition of an equilibrium mixture varies from 35 mole % nitrogen dioxide at 75°F. to nearly 100 mole % nitrogen dioxide at 300°F. Equilibrium is rapidly established in this system (*5*), and therefore maximum effect on thermal properties is obtained. A review of the properties of this system is available in the literature (*3*). Experimental values of thermal conductivity of the system at equilibrium conditions were used in the heat transfer correlation (*3, 6*). Thermal properties of the gas for equilibrium and frozen equilibrium conditions are presented in Figure 1.

The heat transfer rates were determined under turbulent, pipe-flow conditions. Simultaneous mass transfer rates were also determined. The semiempirical relationships used to correlate the data were

$$N_{Nu} = a_1 N_{Re}^{0.8} N_{Pr}^{\frac{1}{3}} \quad (2)$$

for heat transfer (*9*) and

$$N_{Sh} = a_2 N_{Re}^{0.8} N_{Sc}^{\frac{1}{3}} \quad (3)$$

for mass transfer (*9*). The applicability of the correlations and the values for the constants a_1 and a_2 are dependent on the average temperature at which the physical properties of the system that appear in the correlation are evaluated. The determination of this average temperature is the primary problem for this system because of the sensitivity of the physical properties with respect to temperature.

Other heat transfer studies have been performed on this system (*1, 11*).

APPARATUS AND EXPERIMENTAL METHODS

Essential features of the apparatus were heating and cooling sections, a gas pump, flow and temperature measuring devices, and the pressure regulating surge tanks (shown in Figure 2). A closed-cycle system was used in order to eliminate the disposal problem of the toxic and costly nitrogen dioxide. The system was continuously vented during a run to avoid the accumulation of any gaseous products that might be formed by corrosion. Makeup gas was supplied from the isothermal liquid reservoir.

The heater section shown in Figure 3 was a nickel plated copper pipe 49½ in. long with an I.D of 0.563 in. and an O.D. of 0.840 in. Five separate nichrome wire heating elements were wound along the outside surface of the pipe. These were electrically insulated from the pipe by layers of spun glass tape and Saureisen cement. Radial traversing temperature probes and piezometer rings for measuring static pressure were located at four positions along the pipe, 1¾, 10, 29½, and 47¾ in. downstream from the entrance. These positions are, respectively, referred to as stations 1, 2, 3, and 4 in this paper as indicated in Figure 2. At stations 2 and 4 there were also radial traversing total-pressure probes. Wall temperature was measured at seven positions along the pipe by means of chromel-alumel thermocouples imbedded in the pipe wall.

The traversing mechanisms for obtaining radial temperature and total-pressure profiles were spring-loaded, micrometer-activated devices (shown in Figure 3) which could be positioned to within ± 0.0001 in. The radial-probe thermocouples were made of 0.005-in. diameter chromel-alumel wire. The total-pressure tubes were made of 0.025-in. diameter hypodermic tubing. The piezometer rings were hollow rings with a ⅛-in. diameter semicircular cross section and covered a series of four 0.013-in. diameter radial holes in the pipe wall. Both static and total pressures were measured by means of a micromanometer to within ± 0.0002-in. head of kerosene. Thermocouple potentials were measured on a potentiometer which could be read to 10 μv. A watt meter with an accuracy of 0.5% was used to measure the power input to the heaters.

Stainless steel sections representing a length-diameter ratio of 48 to 1 at the entrance and 36 to 1 at the exit preceded and followed respectively the heater sec-

David M. Mason is at Stanford University, Stanford, California.

Tabular material has been deposited as document 6625 with the American Documentation Institute, Photoduplication Service, Library of Congress, Washington 25, D. C., and may be obtained for $5.00 for photoprints or $2.25 for 35-mm. microfilm.

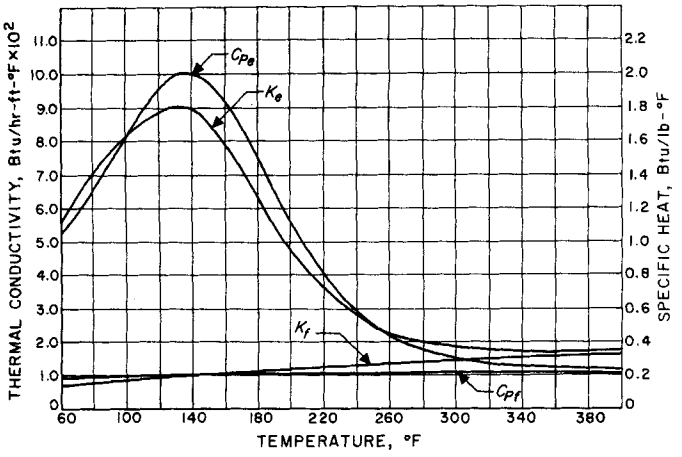

Fig. 1. Thermal properties of the nitrogen dioxide system.

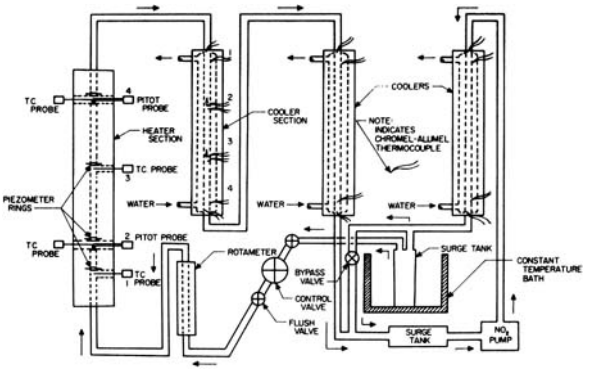

Fig. 2. Heat transfer apparatus.

tion to insure a fully developed velocity profile at the entrance to the heater and to reduce effects of downstream disturbances on flow in the heating section. These sections had the same inside diameter as the heater, and they were indexed with respect to the inside diameter of the heater to insure a smooth junction.

Concentric-tube, countercurrent coolers were used with water flowing in the annular space and gas in the inner tube. Each cooler was 6 ft. in length and was fabricated from 0.049 in. thick stainless steel tubes which were 1 and ⅝-in. O.D. The first cooler downstream from the heater was as shown in Figure 2, equipped with four thermocouple stations at 2-ft. intervals to measure wall and mixed mean-gas temperatures. Inlet and outlet water temperatures were also measured. Water-flow rates were measured with orifice meters. A second cooler was used to cool the gas further before entry to the blower and a third was used to cool the exit gas from the blower. The gas pump was of the positive displacement type and was equipped with upstream and downstream surge tanks.

Flow rates of nitrogen dioxide were measured with a calibrated rotometer. Flow rates were also checked with the bulk velocity calculated from integrated pitot-tube measurements and the agreement between the two methods was within 3%.

The heat transfer tests were made over a Reynolds number range of 6,700 to 22,000 which corresponded to a total mass flow rate of 10 to 25 lb./hr. Wall temperatures for the various tests ranged from 100° to 400°F. The pressure at the entrance to the heater was maintained at 1 atm. by controlling the temperature of the two-phase nitrogen dioxide system in the constant temperature bath shown in Figure 2.

The apparatus was calibrated by using air as the reference gas. Accuracy and response of the thermocouple and pressure probes were checked by obtaining heat transfer coefficients for air. Heat losses were determined at various wall temperatures under zero-flow conditions.

Nitrogen dioxide used in these tests was 99% pure material. The purity was qualitatively checked by freezing a sample of the gas in a liquid nitrogen trap and noting that no residual gas pressure remained and that the color of the solid material was straw yellow. Traces of materials such as nitric acid, nitric oxide, and water will cause the solid to become bluish green. The gas was dried with phosphorous pentoxide and was continuously circulated through this drying agent located in the upstream surge tank.

FROZEN AND REACTION CONTRIBUTION TO EQUILIBRIUM PROPERTIES

The thermochemical and transport properties for the nitrogen dioxide gas tabulated in the literature (3) were obtained directly and indirectly from experimental thermodynamic and spectroscopic data. There is a slight discrepancy between the calculated (3) and the experimental (6) thermal conductivity.

Properties of a reacting system can be characterized as either equilibrium or frozen. Equilibrium thermal properties such as specific heat and thermal conductivity (shown in Figure 1) which involve enthalpy of reaction and rate of change of composition with respect to temperature are greatly temperature dependent. However these properties under frozen equilibrium conditions where composition is fixed do not have the large temperature dependence. Properties such as viscosity (3) and density (10) which are measured under isothermal conditions have the same values under equilibrium and frozen equilibrium conditions.

In analyzing the effect of dissociation on the thermal properties of the system it is assumed that the equilibrium values consist of a frozen and reaction contribution which are linearly additive. With this assumption the equilibrium values of specific heat at constant pressure and thermal conductivity can be written as (4, 8, 11)

$$C_{p_e} = C_{p_f} + C_{p_r} \qquad (4)$$

and

$$k_e = k_f + k_r \qquad (5)$$

The reaction contribution to the specific heat is of the form (4)

$$C_{p_r} = \frac{\Delta H_r}{M_{N_2O_4}} \left.\frac{\partial \alpha}{\partial T}\right|_p \qquad (6)$$

The reaction contribution to the thermal conductivity is due to the diffusion of reaction enthalpy via mass diffusion and is of the form (4)

$$k_r = \frac{D_{12}\rho \Delta H_r}{M_{N_2O_4}} \left.\frac{\partial \alpha}{\partial T}\right|_p \qquad (7)$$

These expressions can be reduced by the use of the assumption of a perfect gas and of the thermodynamic relations of

$$K_p = \frac{4\alpha^2 p}{1-\alpha^2}$$

and

$$\frac{d \ln K_p}{d\frac{1}{T}} = -\frac{\Delta H_r}{R}$$

to the form (4)

$$C_{p_r} = \frac{\alpha(1-\alpha^2)R}{2M_{N_2O_4}} \left(\frac{\Delta H_r}{RT}\right)^2 \qquad (8)$$

and (4)

$$k_r = \frac{\alpha(1-\alpha)}{2} \frac{D_{12}p}{T} \left(\frac{\Delta H_r}{RT}\right)^2 \qquad (9)$$

Values of C_{p_r} and k_r can be estimated from kinetic theory relationships (8).

METHOD OF CORRELATING HEAT AND MASS TRANSFER IN REACTING SYSTEMS

To obtain a correlation of variables in a system in which radial and longitudinal gradients of properties exist it is necessary to establish an effective average state of the system. An average condition for the system was inferred from the heat and mass transfer equations used. The equation for heat transfer is

$$q = 2\pi r_o \int_{z_i}^{z_j} k_{e_w} \left.\frac{\partial T}{\partial y}\right|_w dz \qquad (10)$$

and for mass transfer is (4)

$$N_{N_2O_4} = 2\pi r_o \int_{z_i}^{z_j} \frac{D_{12_w}\rho_w}{M_{N_2O_4}} \left.\frac{\partial \alpha}{\partial y}\right|_w dz \ldots \qquad (11)$$

where

$$y = r_o - r$$

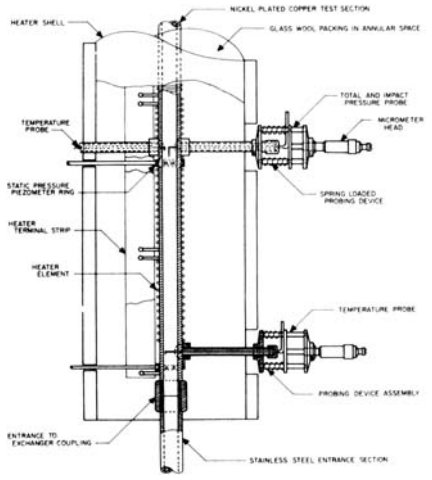

Fig. 3. Heater section.

If the physical properties in Equations (10) and (11) are evaluated at a temperature that is appropriately averaged in the longitudinal and radial directions, and if the laminar sublayer thickness through which most of the resistance to transfer occurs is such that $\delta/d << 1$, giving a flat temperature and composition profile in the turbulent core, then these equations can be written in the form

$$q = 2\pi r_o \frac{k_{e\delta}}{\delta_h} \int_{z_i}^{z_j} (T_w - T_b)\,dz$$

and (12)

$$N_{N_2O_4} = 2\pi r_o \frac{(D_{12}\rho)_\delta}{M_{N_2O_4}\,\delta_M} \int_{z_i}^{z_j} (\alpha_w - \alpha_b)\,dz \ldots \quad (13)$$

The average condition at which the properties denoted by subscript δ must be evaluated is a temperature between the wall temperature and the mixed mean bulk temperature. Such an average temperature which correlates the data well corresponds to the state of the system at the average specific enthalpy, defined as

$$H_\delta = \frac{1}{2(Z_j - Z_i)} \int_{z_i}^{z_j} (H_w + H_b)\,dz \quad (14)$$

The heat transfer coefficient and the mass transfer coefficient are defined by

$$q = 2\pi r_o h \int_{z_1}^{z_j} (T_w - T_b)\,dz$$

and (15)

$$N_{N_2O_4} = 2\pi r_o h' \int_{z_i}^{z_j} (\alpha_w - \alpha_b)\,dz \quad (16)$$

From Equations (12) and (15) the standard form of the Nusselt number results:

$$N_{Nu_e} = \frac{h_e d}{k_{e\delta}} = \frac{d}{\delta_h} \quad (17)$$

Also from Equations (13) and (16) the standard form of the Sherwood number results:

$$N_{Sh} = \frac{h' d}{D_{12\delta}} = \frac{d}{\delta_M} \quad (18)$$

An alternate approach to the heat transfer correlation can be made by assuming that the transfer may be expressed as a sum of two components: a frozen equilibrium component and a transport of reaction enthalpy component. The equation for isobaric heat transfer then becomes, when one substitutes in accordance with Equation (5), k_f, and Equation (7), k_r, into Equation (10):

$$q = 2\pi r_o \int_{z_i}^{z_j} k_{fw} \left.\frac{\partial T}{\partial y}\right|_w dz + 2\pi r_o \int_{z_i}^{z_j} \frac{\Delta H_r}{M_{N_2O_4}} D_{12w}\rho_w \left.\frac{\partial \alpha}{\partial y}\right|_w dz \quad (19)$$

Equation (19) can be written in the form of finite ratios instead of derivatives, and combining with Equation (12) one gets

$$\frac{k_{e\delta}}{\delta_h} \int_{z_i}^{z_j} (T_w - T_b)\,dz = \frac{k_{f\delta}}{\delta_h} \int_{z_i}^{z_j} (T_w - T_b)\,dz + \frac{\Delta H_r}{M_{N_2O_4}} \frac{(D_{12}\rho)_\delta}{\delta_M} \int_{z_i}^{z_j} (\alpha_w - \alpha_b)\,dz \quad (20)$$

or since $h = k_\delta/\delta_h$

$$h_e \int_{z_i}^{z_j} (T_w - T_b)\,dz = h_f \int_{z_i}^{z_j} (T_w - T_b) + \frac{\Delta H_r}{M_{N_2O_4}} \frac{(D_{12}\rho)_\delta}{\delta_M} \int_{z_i}^{z_j} (\alpha_w - \alpha_b)\,dz \quad (21)$$

Equation (21) can be reduced to

$$\frac{h_e}{h_f} = 1 + \frac{\Delta H_r}{M_{N_2O_4}} \left(\frac{D_{12}\rho}{k_f}\right) \frac{\delta_h}{\delta_M}$$

$$\frac{\int_{z_i}^{z_j} (\alpha_w - \alpha_b)\,dz}{\int_{z_i}^{z_j} (T_w - T_b)\,dz} \quad (22)$$

However from Equations (2), (3), (17), and (18), assuming a_1 and a_2 are equal, one obtains

$$\frac{\delta_h}{\delta_M} = \left(\frac{N_{Sc}}{N_{Pr_e}}\right)_\delta^{1/3}$$

and thus Equation (22) becomes

$$\frac{h_e}{h_f} = 1 + \frac{\Delta H_r}{M_{N_2O_4} C_{p_f}} \left(\frac{N_{Pr_f}}{N_{Sc}}\right)_\delta^{2/3} \left(\frac{N_{Pr_f}}{N_{Pr_e}}\right)_\delta^{1/3} \frac{\int_{z_i}^{z_j} (\alpha_w - \alpha_b)\,dz}{\int_{z_i}^{z_j} (T_w - T_b)\,dz} \quad (23)$$

When one uses Equations (4) and (6), Equation (23) may be written as

$$\frac{h_e}{h_f} = 1 + \left(\frac{N_{Pr_f}}{N_{Sc}}\right)_\delta^{2/3} \left(\frac{N_{Pr_f}}{N_{Pr_e}}\right)_\delta^{1/3} \left[\frac{C_{p_e}}{C_{p_f}} - 1\right]_\delta \quad (24)$$

The heat transfer coefficient was determined from Equation (15) with q determined either electrically or from a knowledge of the specific enthalpy profiles:

$$q = m(H_{b_j} - H_{b_i}) \quad (25)$$

Mixed-mean bulk enthalpy at each station was obtained from the point temperature and velocity measurements by use of

$$H_b = \frac{2\pi}{m} \int_o^{r_o} r\, v\rho\, H\, dr \quad (26)$$

The mixed-mean bulk temperature was that temperature corresponding to H_b. As a check the quantity $m(H_{b_4} - H_{b_1})$ was calculated and compared with the measured electrical energy input, the agreement between the two methods being within 5%. The mass flow rate was determined from the point temperature (from which density can be calculated) and velocity measurements by use of

$$m = 2\pi \int_o^{r_o} r\, v\rho\, dr \quad (27)$$

and also from the rotameter measure-

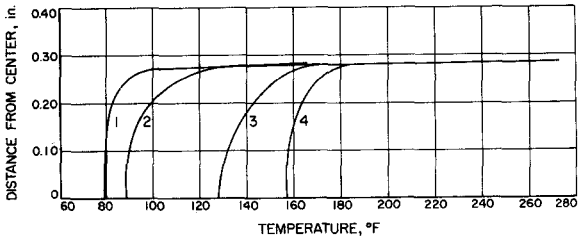

Fig. 4. Typical radial temperature profiles.

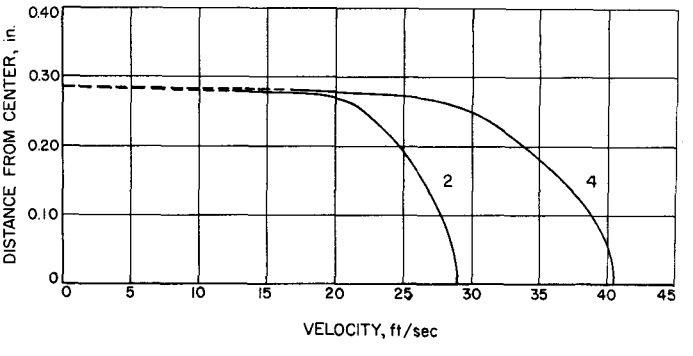

Fig. 5. Typical radial velocity profiles.

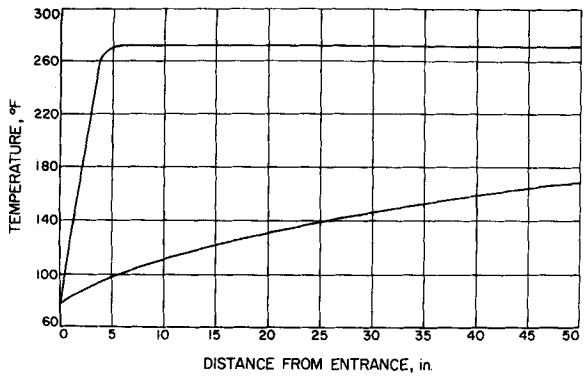

Fig. 6. Typical longitudinal mixed mean gas and wall temperature for heating.

ments; the agreement between the two techniques was within 3%.

The mass transfer coefficient was determined from Equation (16) with

$$N_{N_2O_4} = \frac{m}{M_{N_2O_4}} (\alpha_{bj} - \alpha_{bi}) \quad (28)$$

The fraction dissociated at the wall was assumed to be the equilibrium value corresponding to T_w, and the fraction dissociated for the mixed-mean bulk was assumed to be the equilibrium value at T_b.

The integrations in Equations (14), (15), (16), (26), and (27) were performed graphically with a planimeter.

The frozen equilibrium heat transfer coefficient for this system was calculated from

$$\frac{h_f d}{k_{f\delta}} = a_1 (N_{Re})_\delta^{0.8} (N_{Prf})_\delta^{1/3} \quad (29)$$

EXPERIMENTAL RESULTS

Typical experimental radial temperature profiles are shown in Figure 4, radial velocity profiles in Figure 5, and longitudinal mixed-mean gas and wall temperature profiles in Figure 6.

The heat-transfer coefficients as determined from Equation (15) were correlated in the form of Equation (2). The properties of the system were the equilibrium values evaluated at the average temperature T_δ described in connection with Equation (14):

$$(N_{Nu_e})_\delta = a_1 N_{Re_\delta}^{0.8} (N_{Pr_e})_\delta^{1/3} \quad (2a)$$

A value of 0.018 for a_1 compared with with 0.023 in (9) was obtained from the data which are plotted in Figure 7.

The mass transfer coefficients as determined from Equation (16) were correlated in the form of Equation (3), properties being again evaluated at the average temperature T_δ:

$$N_{Sh_\delta} = a_2 N_{Re_\delta}^{0.8} N_{Sc_\delta}^{1/3} \quad (3a)$$

A value of 0.018 for a_2 compared with 0.023 in (9) was obtained from the data show plotted in Figure 8.

Thus the reacting heat transfer and mass transfer correlations of Figures 7 and 8 follow Equations (2a) and (3a) respectively which are similar to the equations applicable to nonreacting systems (9). Values for the constants a_1 and a_2 of 0.018 fit the reacting data better than the value 0.023 in the literature for nonreacting systems (9). It is noteworthy that if film properties are based on the average of T_b and T_w instead of on T_δ [Equation (14)], much greater scatter of the heat and mass transfer data results. Thus it is advisable to base film properties on the specific enthalpy in accordance with Equation (14).

Heat transfer coefficient ratios as determined from Equations (23) and (24) are presented in Figures 9 and 10, respectively. It is noteworthy that values of h_e/h_f as large as 14 were observed, illustrating the effectiveness of reacting systems as heat transfer media.

The total scatter in the data was of the order of ± 15%. This number reflects the possible errors introduced through the instability in heat input and flow rate that developed during the extended period of time that was required to complete a run, the deviation of pressure from 1 atm. due to the variation of temperature in the surge tank, the accumulation of inert gases in the system due to corrosion, the possibility at the higher wall temperature of side reactions such as

$$NO_2 \rightleftharpoons NO + \frac{1}{2} O_2$$

and the limitations in the analysis and the assumptions. The first two possible sources of errors should in all proba-

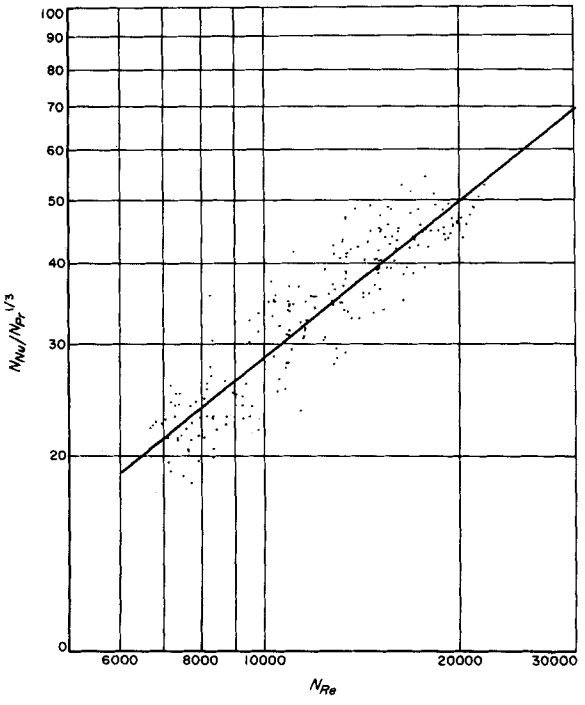

Fig. 7. Heat transfer correlation, Equation (2a).

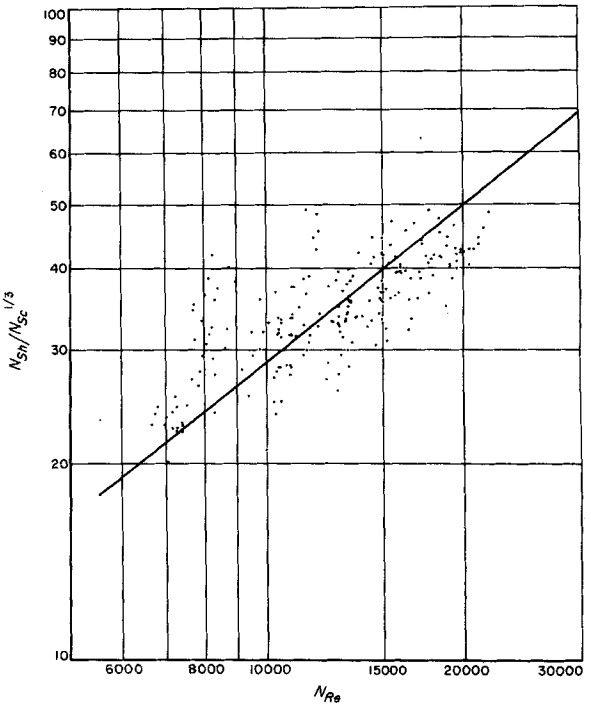

Fig. 8. Mass transfer correlation, Equation (3a).

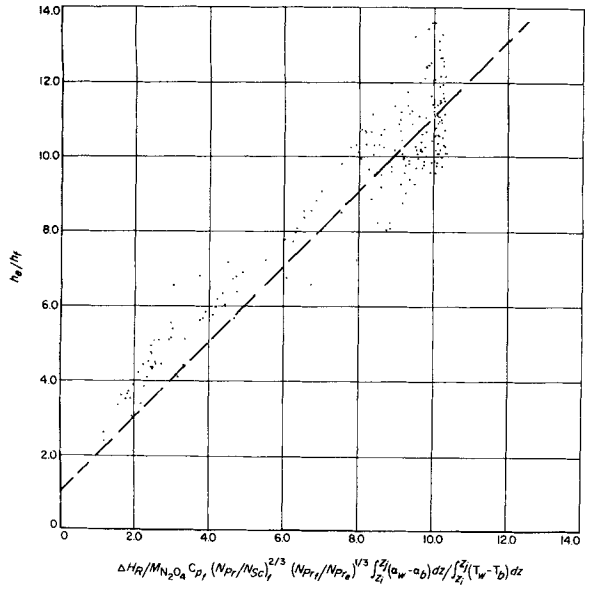

Fig. 9. Effect of dissociation on heat transfer, Equation (23).

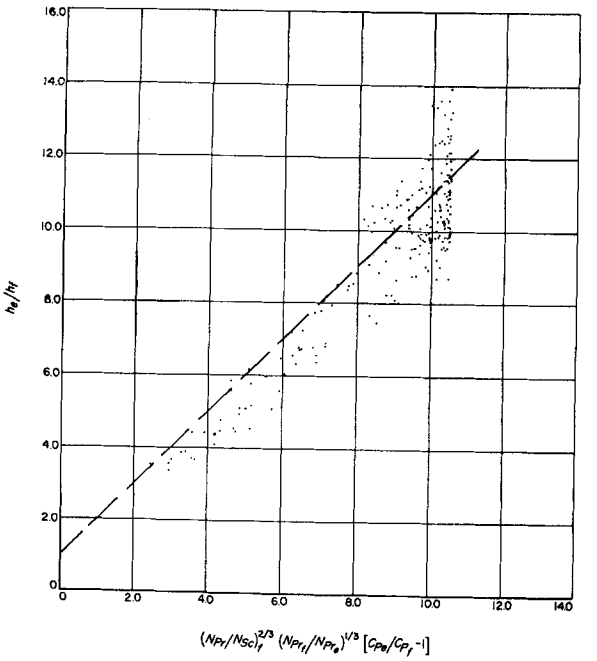

Fig. 10. Effect of dissociation on heat transfer, Equation (24).

bility be random. The effect of the third possible error would depend on the operating temperature. However samples of the material in the apparatus at the beginning and end of each run did not contain any inert gases. The fourth possibility would not produce a random effect. It would cause a higher heat transfer rate to be observed for a given mass transfer rate. This effect is evident in some of the runs made at the highest wall temperatures. However kinetics data for the forward step (2) suggest too slow a reaction to give any measurable effects at the highest temperature studied (400°F.).

CONCLUSIONS

Heat transfer correlations have been developed and experimentally tested for a system that undergoes homogeneous chemical dissociation. The relaxation times for the system were of an order that permitted the assumption of the existence of chemical equilibrium throughout the system.

The net process involved in increasing the heat transfer rate for a homogeneous dissociating system is similar to that of a system that is surface catalyzed and diffusion controlled where the reaction heat is absorbed or liberated at the exchange surface and not transferred through the laminar sublayer. The use of an appropriately averaged film specific enthalpy instead of temperature in determining film properties is experimentally justified.

ACKNOWLEDGMENT

The support of the National Science Foundation under Grants No. G-2425 and G-7327 at Stanford University is gratefully acknowledged in aiding computation and preparation of the manuscript.

NOTATION

A = circumferential transfer area
a = arbitrary constant
C_p = specific heat at constant pressure
d = inner diameter of pipe
D_{12} = binary diffusion coefficient, either molal or volume (9)
h = heat transfer coefficient
h' = mass transfer coefficient
H = specific enthalpy
k = thermal conductivity
K_p = equilibrium constant
m = bulk mass longitudinal flow rate
M = molecular weight
$N_{N_2O_4}$ = radial molal flux of nitrogen dioxide relative to stationary observer
N_{Nu} = Nusselt number, hd/k
N_{Pr} = Prandtl number, $C_p\mu/k$
N_{Re} = Reynolds number $dv\rho/\mu$
N_{Sc} = Schmidt number, $\mu/D_{12}\rho$
N_{Sh} = Sherwood number, $h'd/D_{12}$
p = pressure
q = radial heat flux
r = radial distance
r_o = inner radius of the pipe
R = universal gas constant
T = temperature
y = $(r_o - r)$
v = velocity
z = length

Greek Letters

α = fraction nitrogen dioxide dissociated
ΔH_r = enthalpy of reaction per pound mole of reactant
δ_h = effective heat transfer boundary-layer thickness
δ_M = effective mass transfer boundary-layer thickness
ρ = mass density
μ = viscosity

Subscripts

b = mixed mean bulk condition
e = equilibrium condition
f = frozen equilibrium condition
i = upstream station
j = downstream station
r = contribution due to reaction
w = wall condition
δ = averaged boundary-layer condition

LITERATURE CITED

1. Beal, J. L., and R. L. Lyerly, *Contract No. AF33(616-2954)*, Cornell Aeronautical Laboratory, Inc., Ithaca, New York (September, 1956).
2. Bodenstein, Max, *Z. phys. Chem.*, **100**, 87 (1922).
3. Brokaw, R. S., *Natl. Advisory Comm. Aeronaut. Res. Memo. E57K19a* (March 5, 1958).
4. Butler, J. N., and R. S. Brokaw, *J. Chem. Phys.*, **26**, 1636 (1957).
5. Carrington, T., and N. Davidson, *Phys. Chem.*, **57**, 418 (1953).
6. Coffin, K. P., and J. C. O'Neal, *Natl. Advisory Comm. Aeronaut. Tech. Note 4209* (February, 1958).
7. Hirschfelder, J. O., *J. Chem. Phys.*, **26**, 274 (1957).
8. ———, C. F. Curtiss, and R. B. Bird, "Molecular Theory of Gases and Liquids," Wiley, New York (1954).
9. McCabe, W. L., and J. C. Smith, "Unit Operations of Chemical Engineering," McGraw-Hill, New York (1956).
10. Schlinger, W. G., and B. H. Sage, *Eng. Chem.*, **42**, 2158 (1950).
11. Schotte, William, *Ind. Eng. Chem.*, **50**, 683 (1958).

Manuscript received June 6, 1960; revision received December 9, 1960; paper accepted December 15, 1960. Paper presented at A.I.Ch.E. Salt Lake City meeting.